PHYSICAL REVIEW B VOLUME 26, NUMBER 4 15 AUGUST 1982

Pressure and temperature effects on the thermal conductivity of CuCl

Glen A. Slack
Research and Development Center, General Electric Company, Schenectady, New York 12301

Per Andersson
Department of Physics, University of Umeå, S-901 87 Umeå, Sweden
(Received 25 November 1981)

The thermal conductivity of polycrystalline, cubic CuCl has been measured from 100 to 480 K and pressures from 0.5 to 2.7 GPa by a transient hot-wire technique. The heat transport is produced by phonons. The absolute value of the conductivity is low and becomes nearly temperature independent at high temperatures where it is approaching the minimum possible value. The conductivity decreases with increasing pressure; its volume derivative, g, is negative over the whole range studied. This effect is related to the negative Grüneisen parameters, γ, for the transverse-acoustic phonons. Some specific-heat-capacity values were also measured.

I. INTRODUCTION

The present experiments on CuCl were undertaken in order to determine whether or not this material has a negative-g value, where g is defined as

$$g = -\left[\frac{\partial \ln K}{\partial \ln V}\right]_T .$$

Here K is the thermal conductivity and V the sample volume. Previous experiments on the thermal conductivity[1] of ice and ammonium fluoride had exhibited such negative-g values. All other known crystals had positive-g values. Ice and ammonium fluoride have an adamantine structure and possess a large amount of hydrogen in the structure. It was thought worthwhile to determine whether the hydrogen is a necessary ingredient for obtaining negative-g values. It turns out that it is not. The negative-g values are a consequence of the very open adamantine structure and the negative Grüneisen parameters of the transverse-acoustic modes.[2] Thus CuCl was chosen as a model substance because it has a very large and negative thermal Grüneisen parameter at low temperatures, as determined[3] from thermal expansion measurements. The results on CuCl in the present paper reinforce the arguments for this particular cause of the negative-g values.

II. SAMPLE PREPARATION

The CuCl powder used was commercial reagent-grade material. It was treated in an HCl solution containing excess copper metal in order to remove any $CuCl_2$ and to ensure that only Cu^{1+} was present. The CuCl powder was then carefully dried under vacuum at 520 K. The desired cubic zinc-blende structure is stable[4] up to 680 K. An x-ray analysis of the powder revealed only cubic CuCl with a lattice parameter of $a_0 = 5.418$ Å. Exposure of the powder to moisture was avoided, and it was white in color when installed in the pressure cell. Green $CuCl_2 \cdot 2H_2O$ was not present. Care was also taken to avoid contamination with Cu_2O since it exhibits anomalous[5–7] effects under pressure. The CuCl powder was compressed into two circular discs 39 mm in diameter and 5-mm thick.

III. EXPERIMENTAL TECHNIQUES

The thermal conductivity was measured using the transient hot-wire method. Details of the method and of the general experimental arrangements have been given elsewhere.[8,9] The nickel heater-thermometer wire, 0.1 mm in diameter, was installed as a circular loop between the two CuCl discs in the Teflon-lined pressure cell. The electrical resistivity of CuCl is very high so that the nickel wire was used in direct contact with the sample. The temperature was controlled by either heating or refrigerating the whole massive pressure cell, and it was measured using a Chromel-Alumel thermocouple. The measurements were carried out in the temperature range 100–480 K and at pressures up to 2.7 GPa. The thermal conductivity

was determined with an accuracy of $\pm 3\%$ except at the lowest and highest temperatures where a limit of $\pm 5\%$ must be given. In order to ensure good thermal contact between the hot-wire and the specimen, a minimum pressure of 0.5 GPa was used.

IV. DATA

The basic experimental data are given in Figs. 1 and 2 showing the thermal conductivity K in W/m K as a function of temperature T in kelvin, and as a function of pressure P in gigapascal. We have covered the temperature range from 98 to 479 K and the pressure range from 1 atm (10^{-4} GPa) to 2.7 GPa. Three runs were made at constant pressure while the temperature was varied (Fig. 1), and thirteen runs were made at eight different constant temperatures while varying the pressure (Fig. 2). The data points shown in the graphs in Figs. 1 and 2 are representative. However, each curve is a composite of 200 to 400 data points recorded on an automatic data-taking computer. The experimental data in Fig. 2 can be extrapolated to 10^{-4} GPa (i.e., 1 atm) at constant temperature to yield values of K vs T. These results are shown in Fig. 3. The curves in Fig. 2 also yield a K vs T curve at 2.5 GPa.

CuCl undergoes various structural changes under pressure.[4,10–14] At room temperature these changes all occur at or above pressures of 4 GPa. We have been careful to avoid these phase changes, and the present samples were all in the phase with the zinc-blende structure.

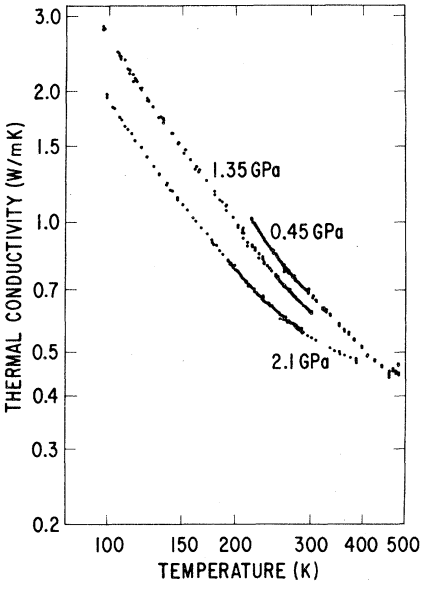

FIG. 1. Thermal conductivity vs temperature at three isobars.

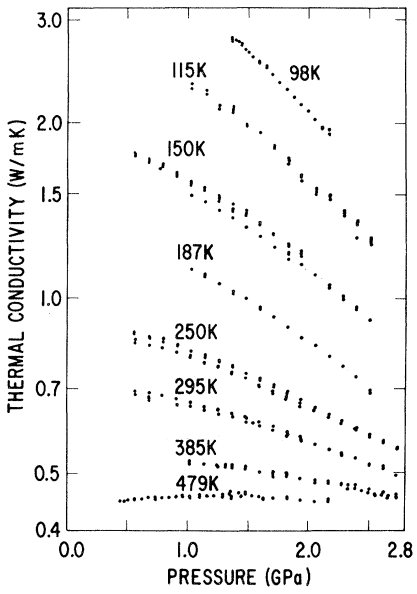

FIG. 2. Thermal conductivity vs pressure at eight different isotherms.

V. ANALYSIS OF THE RESULTS

Phonons are the dominant heat carriers in CuCl. The electrical resistance was so high that electron

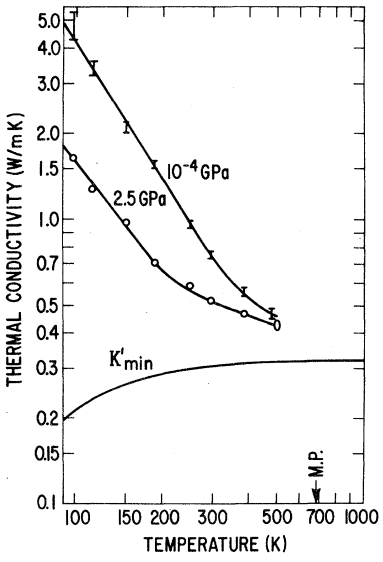

FIG. 3. Thermal conductivity vs temperature at 10^{-4} and 2.5 GPa. The curve labeled $K'_{\min}$ is the theoretical value of the minimum thermal conductivity.

heat transport is negligible. The results in Figs. 1–3 can be analyzed using the theoretical models of Slack.[15] This reference will be referred to as SSP [*Solid State Physics* (Ref. 15)]. For such an analysis values are needed for the acoustic Debye temperature $\tilde{\Theta}$, the Grüneisen parameter γ, the predicted minimum thermal conductivity $K'_{\min}$, as well as a knowledge of the crystal structure and the phonon dispersion curves.[16–18]

A. Acoustic Debye temperatures

As explained in SSP the Debye temperature in the high-temperature limit $\tilde{\Theta}_\infty$ can be obtained from the phonon density of states $g(\nu)$. Equation (1.3) of SSP gives

$$\tilde{\Theta}_\infty = \frac{h}{k}\left[\tfrac{5}{3}\int_0^\infty \nu^2 g(\nu)d\nu \Big/ \int_0^\infty g(\nu)d\nu\right]^{1/2}, \tag{1}$$

where h is Planck's constant, k is Boltzmann's constant, and ν is the phonon frequency. The tilde over the Θ indicates that the integration is over the acoustic modes only. In CuCl the large atomic mass ratio of 1.8 separates the optic and acoustic modes quite well.[17] In fact the transverse- and longitudinal-acoustic modes are also well separated.[17] The $g(\nu)$ curves of Prevot *et al.*[17] at 4.2 K were integrated to obtain

TABLE I. Phonon frequencies, characteristic temperatures, and Grüneisen parameters.

Phonon branch	ν (THz)	Θ (K)	Group velocity (10^5 cm/sec)	γ
TA	1.50 (max)	73	1.49	−2.5
LA	3.75 (max)	193	3.53	+2.0
TO	6.2	300	~0	+2.4
LO	6.96	335	~0	+3.0

$$\begin{aligned}\tilde{\Theta}_\infty(\mathrm{TA}) &= 73\ , \\ \tilde{\Theta}_\infty(\mathrm{LA}) &= 193\ ,\end{aligned} \tag{2}$$

in units of K. These values are given in Table I. An average $\tilde{\Theta}$ for all the acoustic modes is given by

$$\begin{aligned}\tilde{\Theta}_\infty &= \{\tfrac{2}{3}[\tilde{\Theta}_\infty(\mathrm{TA})]^2 + \tfrac{1}{3}[\tilde{\Theta}_\infty(\mathrm{LA})]^2\}^{1/2}\ , \\ \tilde{\Theta}_\infty &= 126\ ,\end{aligned} \tag{3}$$

the latter in units of K. The acoustic mode $\tilde{\Theta}$ at absolute zero can be obtained from Eq. (3.4) of SSP,

$$\tilde{\Theta}_0 = \Theta_0 n^{-1/3}\ , \tag{4}$$

where $n=2$, the number of atoms in the primitive unit cell. Using $\Theta_0 = 179$ K from Barron *et al.*[3] we obtain

TABLE II. Contributions to the minimum thermal conductivity in the high-temperature limit.

Modes	$K'_{\min\infty}$ (W/mK)	Fractional contribution	Propagation velocity[a] (10^5 cm/sec)
Propagating			
TA	0.0437	0.140	1.49
LA	0.0576	0.184	3.53
Slowly propagating			
TA	0.0209	0.067	0.40
LA	0.0261	0.083	0.96
TO	0.1054	0.337	1.7
LO	0.0591	0.189	1.9
Total	0.3128	1.000	

[a]This velocity for the slowly propagating phonons is just $\nu\delta$, for the others it is the group velocity.

$$\tilde{\Theta}_0 = 142 \ , \tag{5}$$

in units of K. Note that Vardeny *et al.*[19] find $\Theta_0 = 164$ K. The ratio $\tilde{\Theta}_0/\tilde{\Theta}_\infty = 1.13$ for CuCl. This is very similar to the values found for other zinc-blende crystals in Table II of SSP. In ZnS, which has almost the same masses and mass ratio as CuCl, $\tilde{\Theta}_0/\tilde{\Theta}_\infty = 1.17$.

B. Absolute value of K'

As shown in SSP it is possible to make a reasonable estimate of the value to be expected for the thermal conductivity at the acoustic Debye temperature. Equation (3.3) of SSP gives

$$K'(\tilde{\Theta}_\infty) = Bn^{1/3}\bar{M}\delta(\tilde{\Theta}_\infty)^2\tilde{\gamma}_\infty^{-2} \ , \tag{6}$$

where $B = 3.04\times 10^{+7}$ W/kg m^2 K^3, $\bar{M}$ is the average atomic mass, δ is the average interatomic spacing, and $\tilde{\gamma}_\infty$ is the Grüneisen parameter for the acoustic phonons in the high-temperature limit. If we take the average of γ^2 for the propagating acoustic phonons, we find

$$\bar{\gamma}^2 = \frac{(2\gamma_{\rm TA}^2 + \gamma_{\rm LA}^2)}{3} = 5.5 \tag{7}$$

using the γ values in Table I. This yields

$$K'(126 \text{ K}) = 1.48 \ ,$$

in units of W/mK at $P = 1$ atm. The measured value is 2.9 W/mK from Fig. 3, about twice as large as the calculated estimate. The observed value minus $K'_{\rm corr}$ is 2.7 W/mK (see Sec. V E). The agreement between Eq. (6) and the observed K value is within the limits found for other materials in SSP.

C. Calculated minimum thermal conductivity

The concept of and method of calculating the minimum value of K has been given in SSP. The minimum K is independent of temperature for $T \gg \Theta$, and is

$$K'_{\min\infty}(\text{total}) = K'_{\min A\infty} + K'_{\min O\infty} \ . \tag{8}$$

The A term is for acoustic phonons and the O term is for three combined optic-phonon branches, all at frequency $\nu_{\rm op}$. The optic term is

$$K'_{\min O\infty} = \frac{k\nu_{\rm op}}{n\delta} \ , \tag{9}$$

where $n = 2$. For the optic modes the frequencies and characteristic temperatures are related by

$$h\nu_{\rm op} = k\Theta_{\rm op} \ . \tag{10}$$

Values of $\Theta_{\rm op}$ are given in Table I, and are taken from the neutron scattering results[19] at 4.2 K. The shift in Θ values with temperature is ignored. For the acoustic modes the characteristic temperatures are the $\tilde{\Theta}_\infty$ values derived earlier. The ν_A values are the maximum frequencies of possible phonons for the whole mode. They are taken from the calculated one-phonon density of states of Prevot *et al.*[17] The ν_A values are close to but not identical to the values of $k\tilde{\Theta}_\infty/h$. The average propagation velocities in Table I of the TA and LA modes have been estimated from the Voigt-Reuss-Hill averages of the elastic constants.[20] Using the c_{ij} of Hanson *et al.*[2] this gives, at 300 K, the adiabatic bulk modulus

$$B_s = 39.3 \ ,$$

and the adiabatic shear modulus

$$S_s = 9.13 \ ,$$

both in units of GPa.

1. *Phonon wavelength cutoff*

It can be seen from the phonon dispersion curves[17] that not all of the acoustic phonons have the propagation velocities given in Table I for the lowest-frequency phonons near the zone center. There is some cutoff wavelength, and acoustic phonons of shorter wavelengths can be assumed to have zero propagation velocity. This type of analysis has been employed by Holland[21] for Si and Ge. Phonons of longer wavelengths are assumed to have a constant velocity. This cutoff wavelength for the acoustic phonons is

$$\lambda_c = v/\nu_{\max} \ . \tag{11}$$

These values are, then, for the TA modes,

$$\lambda_c = 9.93 \ ,$$

and for the LA modes,

$$\lambda_c = 9.41 \ , \tag{12}$$

in units of Å. This wavelength cutoff corresponds to a wave-vector cutoff q_c of

$$q_c = 2\pi/\lambda_c \ . \tag{13}$$

The distance from the center to the edge of the first Brillouin zone (BZ) in the [100] direction is $q_{\max}([100])=2\pi/a_0$, where $a_0=5.418$ Å. The average radius of the first BZ is just

$$\bar{q}_{\max}=(3/\pi)^{1/3}q_{\max}([100]) , \tag{14}$$

and $4\pi(\bar{q}_{\max})^3/3$ is the volume of the first zone. The number of phonon modes between the zone center and q_c is proportional to the volume of the first BZ sphere of radius q_c. Hence the fraction of the phonon modes that can transport heat in CuCl is given by

$$\mathcal{F}_t=(q_c/\bar{q}_{\max})^3 , \tag{15}$$

where $\mathcal{F}_t$ is the transport fraction. From Eqs. (11), (12), (13), and (14) this is

$$\begin{aligned}\mathcal{F}_t\ (\mathrm{TA})&=(0.554)^3=0.170 ,\\ \mathcal{F}_t\ (\mathrm{LA})&=(0.585)^3=0.200 .\end{aligned} \tag{16}$$

Thus only about 18% of all the possible acoustic-phonon modes can actually transport heat in CuCl. The other phonons have very small or zero group velocities. This is basically why the thermal conductivity of CuCl is so low. The optic modes in CuCl have such low group velocities that they effectively carry no heat either; see SSP.

2. *Minimum conductivity*

The method in SSP of estimating the minimum thermal conductivity is to give all of those propagating phonon modes with $\lambda>\lambda_c$ a mean free path equal to one wavelength. For the other acoustic modes and optic modes, which are nonpropagating, a mean free path of magnitude δ is assumed. For each propagating acoustic branch the contribution to $K'_{\min}$ is given by

$$K'_{\min A\infty}=\frac{2\pi}{3n}\left[\frac{k}{v}\right]\nu_{\max}^2 . \tag{17}$$

This is obtained by integrating

$$K'=\tfrac{1}{3}\int lvC(\nu)dq ,$$

which is

$$K'=\frac{1}{6\pi^2}\int_0^{q_c}\frac{vl}{n}\left[\frac{kx^2e^x}{(e^x-1)^2}\right]q^2dq . \tag{18}$$

Here $l=\lambda=2\pi/q$, $x=h\nu/kT$, and $C(\nu)=kx^2e^x(e^2-1)^{-2}$ is the heat capacity. For $q\le q_c$ one has

$$v=2\pi\nu/q . \tag{19}$$

For $q>q_c$ one has $v=0$. In the high-temperature limit Eq. (18) becomes Eq. (17). The results are given in Table II. Note that there are two TA branches so that the results of Eq. (17) are doubled for the propagating TA modes.

For the nonpropagating regions of the acoustic modes the expression for $K'_{\min A\infty}$ for a single phonon branch is

$$K'_{\min A\infty}=\left[\frac{k\nu_{\max}}{3n\delta}\right](1-\mathcal{F}_t) . \tag{20}$$

The term in parentheses gives the fraction of the modes, all with frequency $\nu_{\max}$, that have zero group velocity. They then transport energy by an atom-to-atom collision at an effective velocity of $\nu_{\max}\delta$; see Eq. (20.2) of SSP. The optic-mode contributions are given directly by Eq. (9). The sum of all these contributions is

$$K'_{\min\infty}=0.313 ,$$

in units of W/mK. Of this 47% is contributed by the acoustic modes and 53% by the optic modes; see Table II. The temperature dependence of $K'_{\min}$ is given by Eqs. (19.5) and (20.4) of SSP for the propagating and nonpropagating fractions, respectively. The results are shown in Fig. 3. An empirical fit to these results gives K vs T for the limited region $100\le T<\infty$ as approximately

$$K'_{\min}(T)\cong K'_{\min\infty}\left[1-\left[\frac{57}{T}\right]^{1.75}\right] . \tag{21}$$

3. *Minimum conductivity versus pressure*

In order to compare the theory with the experimental results obtained under pressure, it is necessary to calculate how $K'_{\min}$ depends on pressure. This can be done using Eqs. (9), (17), and (20), the γ values from Table I, and the fractional contributions from Table II. The result is

$$K'_{\min\infty}(P)=[K'_{\min\infty}(P=0)][1+(GP/B_T)] , \tag{22}$$

where G is the volume derivative

$$G=\left[\frac{\partial\ln K'_{\min\infty}}{\partial\ln V}\right]_T . \tag{23}$$

The value of G is given by

$$G=\gamma_{TA}(0.140)+(\gamma_{TA}-0.333)(0.067)+\gamma_{LA}(0.184)+(\gamma_{LA}-0.333)(0.083)$$
$$+(\gamma_{TO}-0.333)(0.337)+(\gamma_{LO}-0.333)(0.189)\ . \quad (24)$$

The 0.333 term is just $(\partial \ln\delta/\partial \ln V)=\frac{1}{3}$. The result is

$$G=+1.17\ .$$

The isothermal bulk modulus B_T is calculated to be 40 GPa from data[2,14,22] in the literature, and is assumed to be independent of temperature and pressure. The resultant pressure dependence of $K'_{\min\infty}$ is shown later in Fig. 5.

D. Experimental minimum thermal conductivity

The experimental results in Figs. 1 and 3 have the general form

$$K=[A/T^{\epsilon})+K_{\min}\ . \quad (25)$$

The minimum conductivity appears as a term added to the "normal" temperature-dependent conductivity. The experimental data have been plotted as K vs $T^{-\epsilon}$ in Fig. 4 using the "best-fit" value of $\epsilon=1.75$. These results can be extrapolated to $T=\infty$ readily to give $K_{\min\infty}$ for various pressures as shown in Fig. 5. Two other points derived from Fig. 2 are also given. At $P=1$ atm the experimental value of

$$K_{\min\infty}=0.29\frac{+0.01}{-0.06}\ ,$$

in units of W/mK. The theoretical value is 0.313 W/mK, calculated with no adjustable parameters from the known dispersion curves. The experimental results in Fig. 5 indicate that the theoretical pressure dependence from Eq. (22) is also substantially correct. The $K'_{\min}$ term is thus approximately expressible by

$$K'_{\min}=0.313[1-(57/T)^{1.75}](1+0.029P)\ , \quad (26)$$

in units of W/mK for $100\leq T<\infty$.

E. Propagating acoustic phonons

We shall define the normally propagating acoustic phonons as those that have sonic velocities v; slowly propagating phonons have velocities $v\delta$ and move by atom-to-atom collisions. The temperature and pressure dependence of the heat transport produced by the slowly propagating phonons is small and comparable to that of $K'_{\min}$. The normally propagating acoustic phonons account for most of the pressure and temperature dependence seen in Figs. 1–3. The propagation velocities of these two different groups are given in Table II. In order to correctly analyze this behavior we need to subtract from the total measured thermal conductivity the contribution supplied by the slowly propagating phonons. This correction term is equal to $K'_{\min}$ minus the minimum thermal conductivity of the normally propagating TA and LA modes. This term is thus

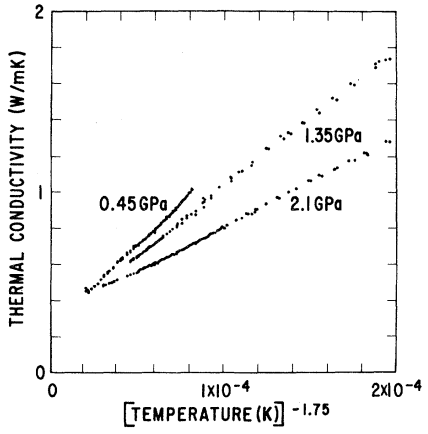

FIG. 4. Thermal conductivity vs $T^{-1.75}$ at three different isobars.

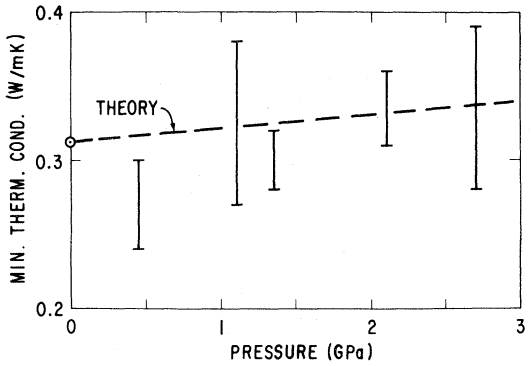

FIG. 5. Extrapolated minimum thermal conductivity vs pressure for five isobars. The dashed line gives the theoretically calculated value.

$$K'_{\text{corr}} \approx 0.211 \left[1 - \left[\frac{62}{T} \right]^{1.72} \right] (1+0.043P) , \tag{27}$$

again in W/mK. This differs slightly from Eq. (26). Further analysis is carried out using

$$K_R = K - K'_{\text{corr}} ,$$

where K is the measured thermal conductivity and K_R is the experimental value for the thermal conductivity of the propagating phonons. In Fig. 6 the curves for K_R vs T are given. Notice especially the effect of K'_{corr} at high temperatures by comparing Fig. 1 with Fig. 6.

F. Temperature dependence of K_R

In the temperature range of 100 to 200 K the temperature dependence of K_R is given by

$$\epsilon = - \left[\frac{\partial \ln K_R}{\partial \ln T} \right]_P , \tag{28}$$

with a value of $\epsilon = 1.6 \pm 0.1$ for pressures of 1.35 and 2.1 GPa. The ϵ value of 1.6 gives the true temperature dependence of K_R. The exponent of -1.75 used in Fig. 4 is an empirical value used to produce a nearly linear extrapolation to $T = \infty$ in order to find experimental values for $K_{\min\infty}$. The large (i.e., > 1.5) value of ϵ makes it appear plausible that there is little or no scattering of the phonons at grain boundaries in the present polycrystalline samples. The measured grain size was about 10 μ, the average mean free path at 100 K due to phonon-phonon scattering is about 0.05 μ. Thus our polycrystalline samples behave almost like single-crystal ones. From SSP we note that the three-phonon acoustic-acoustic scattering predicts $\epsilon = 1.00$. Two possible mechanisms are given in SSP whereby ϵ can be increased above unity; these are thermal expansion and optic-mode scattering. Thus from Eq. (12.5) of SSP,

$$\epsilon = 1.00 + \eta_{\text{th}} + \eta_{\text{op}} . \tag{29}$$

The linear thermal expansion coefficient α vs T as obtained from literature[3,23–25] data is shown in Fig. 7. Values of α, g, and η_{th} are given in Table III. The g values are experimental ones from Fig. 9. The values of η_{th} are given by Eq. (11.3) of SSP. We have

$$\eta_{\text{th}} = 3\alpha g T . \tag{30}$$

Since the g values are negative the η_{th} values are negative. They are also small, and it appears that $\eta_{\text{op}} \approx 0.6$ experimentally.

It is possible to estimate the η_{op} contribution to the value of ϵ. We assume that the 82% of the acoustic modes, those that are nonpropagating and have high peaks in the density of states at 73 and 193 K, scatter the propagating acoustic phonons in a manner similar to that of the optic modes. The coupling constant here is $S = 1$, however, since the scattering is acoustic-acoustic. The η_{op}(acoustic) contribution is given by

$$\eta_{\text{op}}(\text{acoustic}) = 0.82(2Y_{\text{TA}} + Y_{\text{LA}}) , \tag{31}$$

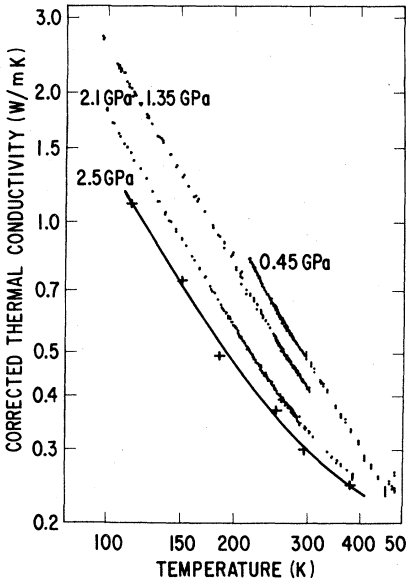

FIG. 6. Corrected thermal conductivity vs temperature at four isobars.

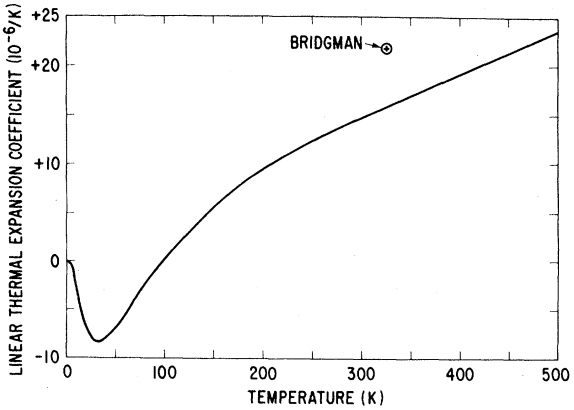

FIG. 7. Linear thermal expansion coefficient as a function of temperature.

TABLE III. Thermal expansion contributions to ϵ.

T (K)	α (10^{-6}K)	g	η_{th}
100	0.0	−22.3	0.000
200	+ 9.3	−17.5	−0.098
300	+ 14.6	−12.6	−0.166
400	+ 19.0	−7.8	−0.178

$$Y_i=\frac{S_i(Z_i+X_i-1)}{3[S_i+(1/Z_i)]}\ ,\quad X_i=\left[\frac{\Theta_i}{T}\right]\ ,$$
$$Z_i=X_i/(e^{X_i}-1)\ . \tag{32}$$

These equations appear in SSP as Eq. (12.4). Similarly the optic-mode contribution is

$$\eta_{\text{op}}(\text{optic})=(2Y_{\text{TO}}+Y_{\text{LO}})\ . \tag{33}$$

The overall η_{op} is just

$$\eta_{\text{op}}=\eta_{\text{op}}(\text{acoustic})+\eta_{\text{op}}(\text{optic})\ . \tag{34}$$

The derived value of $S_{\text{op}}=1.75$, where S_{op} is the scattering strength of the optic phonons relative to that of the acoustic phonons. This means that the scattering of acoustic phonons by optic phonons is 75% stronger than the acoustic-acoustic scattering. This value should not be taken too seriously, but it does indicate that the propagating phonons are scattered by the slowly propagating phonons as well as by interaction with the normal acoustic phonons. This additional scattering by the slow phonons is probably responsible for ϵ being noticeably greater than unity.

G. Volume dependence of K_R

In Fig. 8 we show the results of $\ln(K_R)$ plotted versus $\ln(V/V_0)$. The applied pressure has been converted to a volume change by assuming that the isothermal bulk modulus is $B_T=40.0$ GPa. The slopes of the $\ln(K_R)$ vs $\ln(V/V_0)$ curves between 1.5 and 2.7 GPa are the measured g values given in Table IV and plotted in Fig. 9 as a function of temperature. The value of g appears to increase linearly with increasing temperature from a value of about −22 at 100 K to zero at 560 K. We would like to be able to compare these measured g values with theoretical estimates. The g value at high temperatures can be estimated from K_{min} using the contributions only from the propagating

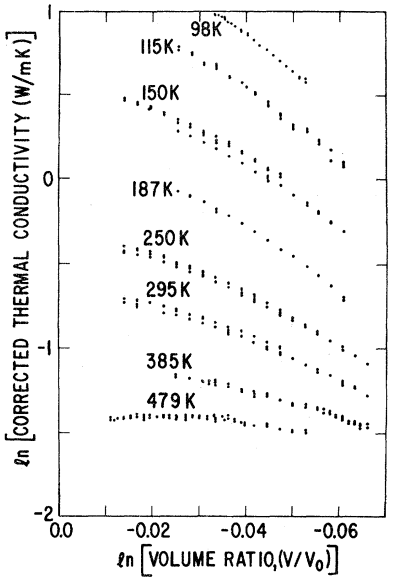

FIG. 8. Corrected thermal conductivity vs sample volume for eight isotherms. The natural logarithms of the values are plotted. Thus the slopes of the curves give the value of g.

TA and LA modes. Thus for $T\gg 193$ or 73 K, the effective Debye temperatures of these modes, we obtain from Eq. (24),

$$g_\infty=\frac{\gamma_{\text{TA}}(0.140)+\gamma_{\text{LA}}(0.184)}{0.140+0.184}\ . \tag{35}$$

Using $\gamma_{\text{TA}}=-2.5$, $\gamma_{\text{LA}}=+2.0$, we find

$$g_\infty=+0.056\ .$$

Thus the high-temperature limit of g is very nearly zero because the negative effect of γ_{TA} cancels the positive effect of γ_{LA}. As the temperature decreases below 193 K, the LA Debye temperature, the contribution of the TA modes begins to exceed that of the LA modes and g should become more and more negative. At 73 K the TA modes dominate the behavior and $g\cong -24$. The value of g is approximately[1] equal to

$$g=5\gamma-\tfrac{1}{3}\ . \tag{36}$$

Thus at 73 K one obtains $\gamma_{\text{TA}}\sim -5$. From reference to Fig. 13 it is apparent that γ_{TA} ($T=0$) is −2.5. This is the average γ_{TA} for phonons near the zone center. For the higher-energy TA phonons it appears that γ decreases to values of about −5 for wave vectors about halfway across the BZ. This observation needs further confirmation, but rather large negative-γ_{TA} values have been calculated[26–28] and measured[29–32] for other diamond or

TABLE IV. Experimental g values in the pressure range 1.5–2.7 GPa.

T (K)	$-g$
98	22.5±0.5
115	21.0±0.5
150	19 ±1
187	18 ±1
250	16 ±1
295	13.0±0.5
385	7.3±0.5
479	4.0±0.5

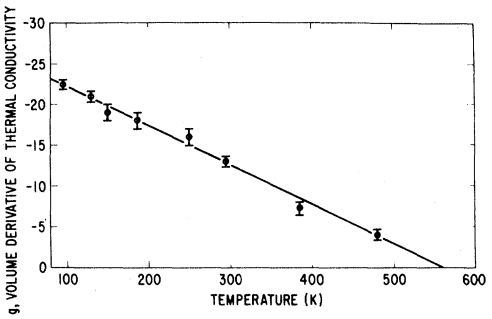

FIG. 9. Volume derivative of K, which is g, vs temperature. The error bars are the estimated uncertainty in the slopes of the lines in Fig. 8.

zinc-blende structure crystals. In CuCl the zone-boundary TA (X) phonons[30] have a $\gamma=-1.7$ while in $AgGaS_2$ the value[32] for some TA modes is $\gamma=-4.4$.

H. Specific-heat capacity

The transient hot-wire method used in the present experiments also yields data for the specific-heat capacity per unit volume as a function of temperature and pressure. If we define C_p as the specific-heat capacity per unit mass at constant pressure and ρ as the mass per unit volume, the specific-heat capacity per unit volume at constant pressure is just ρC_p. This is the quantity measured in the present experiments. Figure 10 gives the results at $P=2.1$ GPa over the temperature range studied. The maximum scatter in the data is about ±7% from the average value. The absolute uncertainty in the values is about ±10%.

In order to compare Fig. 10 with previous results[19] at 1 atm it is necessary to know the pressure dependence of ρC_p. Results for three temperatures are shown in Fig. 11. The expected pressure dependence can be calculated from the following. The specific-heat capacity per unit mass at constant volume C_v is given by

$$C_v = C_{v\infty}\left[\frac{2D(\tilde{\Theta}_{TA})+D(\tilde{\Theta}_{LA})+2E(\Theta_{TO})+E(\Theta_{LO})}{6}\right]. \tag{37}$$

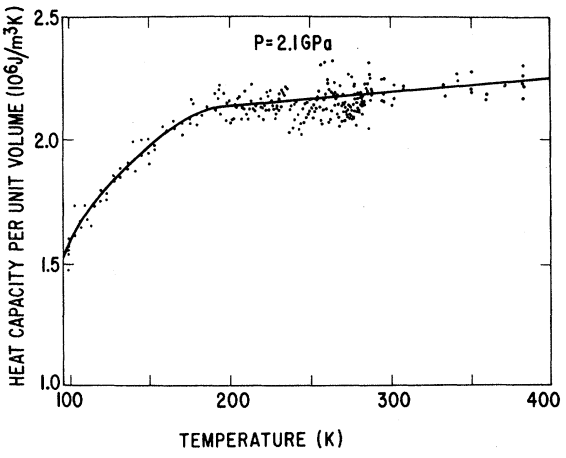

FIG. 10. Heat capacity per unit volume vs temperature at a constant pressure of 2.1 GPa.

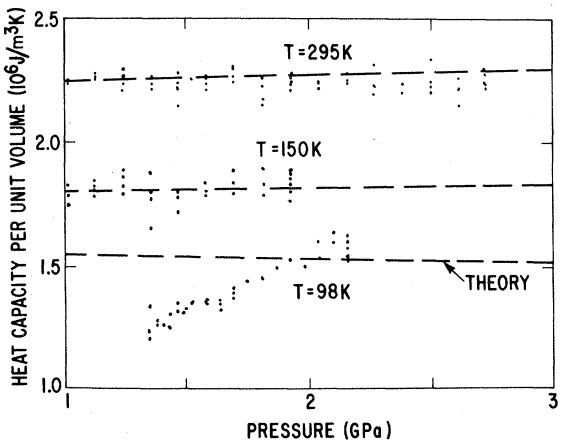

FIG. 11. Pressure dependence of the heat capacity per unit volume at three temperatures. The dashed lines are the theoretical estimates for the pressure dependence.

TABLE V. Calculated pressure dependence of ρC_p.

T (K)	$\partial\ln(\rho C_p)/\partial P$ (GPa^{-1})
100	−0.63%
150	+0.74%
200	+0.92%
300	+1.39%
400	+1.96%
∞	+2.50%

The Θ values are given in Table I. The Θ values change with pressure (or volume) according to

$$\gamma=-\left[\frac{\partial\ln\Theta}{\partial\ln v}\right]_T=-B_T\left[\frac{\partial\ln\Theta}{\partial P}\right]_T, \tag{38}$$

where the γ values in Table I are used. The C_p and C_v are related by

$$C_p/C_v=1+3\alpha\gamma T . \tag{39}$$

Since $3\alpha\gamma T$ is small for CuCl up to 400 K, then

$$\frac{\partial C_P}{\partial P}\cong\frac{\partial C_v}{\partial P} . \tag{40}$$

The overall result is that

$$\frac{\partial\ln(\rho C_p)}{\partial P}\cong+\frac{1}{B_T}\left[1-\frac{\partial\ln C_v}{\partial\ln V}\right] . \tag{41}$$

At the very highest temperature C_v is a constant independent of volume. Hence

$$\frac{\partial\ln(\rho C_p)}{\partial P}=B_T^{-1} .$$

Since $B_T=40$ GPa, $B_T^{-1}=+2.5\%/\text{GPa}$. At lower temperatures the $\partial\ln C_v/\partial\ln V$ term comes in, and the results are given in Table V. These calculated pressure dependencies are also shown in Fig. 11. The agreement for temperatures of 295 and 150 K is very good. The results for 98 K below 2.0 GPa are seen to be suspect and are ignored henceforth. Large differential thermal contraction stresses in the teflon cell and the sample are thought to be influencing the results at these lowest temperatures. The data in Fig. 11 are then corrected to 1 atm pressure and plotted in Fig. 12. A density ρ of 4.132 g/cm^3 has been used.

The present results are about 5% higher than the more accurate data of Vardeny *et al.*[19] below 160 K. This is within the accuracy of the present method. Thus the present results were decreased by 5% and the dashed line in Fig. 12 shows the expected behavior of CuCl up to 400 K. At 400 K the value of $C_p=49.1$ J/mole K. Using Eq. (39) this gives $C_v=47.9$ J/mole K, which is 96% of the Dulong-Petit value of $6R$ at infinite temperature.

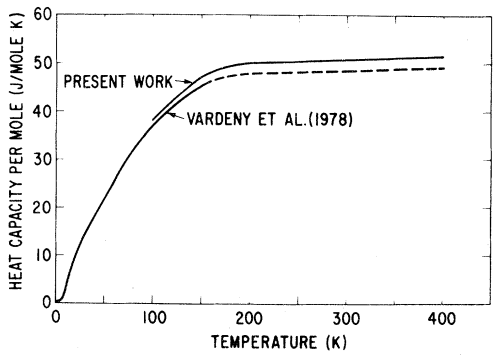

FIG. 12. Heat capacity per mole vs temperature for atmospheric pressure.

TABLE VI. Experimental values of the thermal Grüneisen parameter at various temperatures.

T (K)	γ^{th}
100	0.00
150	0.38
180	0.50
200	0.60
250	0.75
300	0.89
350	1.02
400	1.14
450	1.27
500	1.40

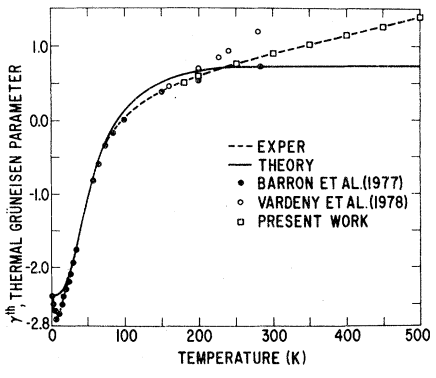

FIG. 13. Thermal Grüneisen parameter vs temperature. The points are experimental data, the solid curve is the theoretical fit.

Thus the dashed extrapolation in Fig. 12 appears to be reasonably accurate. This curve is used in Fig. 13 to calculate γ^{th} vs T.

VI. GRÜNEISEN PARAMETERS AND THERMAL EXPANSION

Some data exist in the literature for the Grüneisen parameters γ of CuCl. Single-mode γ values near the center of the phonon BZ have been determined ultrasonically[2] under pressure. Some values at the zone boundary have been determined by optical experiments[30] under pressure. Previous plots of the thermal Grüneisen parameter γ^{th}, versus T, exist.[3,19] We have determined γ^{th} (see Table VI) from a combination of the thermal expansion (see Fig. 7) and the specific-heat capacity (see Fig. 12). The γ^{th} vs T curve has been fitted by using the selection of mode γ values and Debye temperatures listed in Table I. The fit is shown in Fig. 13. Except for the minimum at 7 K the fit is rather good. The expression used is given by

$$\gamma^{\text{th}}=\frac{2\gamma_{\text{TA}}D(73)+\gamma_{\text{LA}}D(193)+2\gamma_{\text{TO}}E(300)+\gamma_{\text{LO}}E(335)}{2D(73)+D(193)+2E(300)+E(335)} . \tag{42}$$

Here $D(T)$ and $E(T)$ are the Debye and Einstein specific-heat-capacity functions for the given temperature.

Clearly it is an oversimplification to assume that the γ for a particular mode is constant across the whole BZ. Lattice-dynamical calculations[26–28] show that this is not, in general, the case. The minimum at 7 K in Fig. 13 indicates that γ_{TA} is varying rather rapidly as one proceeds outward from the zone center. However, we are mainly interested in the order of magnitude and sign of the mode γs. For this Table I is adequate. These values have been used in the preceding parts of this paper.

VII. AVERAGE PHONON LIFETIMES

Several studies of the vibrations or excursions of the Cu and Cl ions from their equilibrium positions show large motions. This can be interpreted as large excursions into the regions where the anharmonic terms in the interatomic potential become very important. Evidence for the rapid decrease of the mean lifetime of the lattice phonons with increasing temperature comes from the neutron scattering studies.[16,17] Prevot *et al.*[17] find that for $T>200$ K many of the phonon peaks are too broad to be seen. At 200 K and 1 atm pressure the measured K is about 5 times its minimum value. Hence the mean free path of these propagating phonons is five wavelengths. In terms of the phonon frequency this means for the dominant acoustic phonons,

$$\nu\tau=5 , \tag{43}$$

at 200 K, where τ is the lifetime. At 200 K the higher-energy acoustic phonons will be the dominant carriers. These will be in the frequency range of 1 to 4 THz (see Table I). Thus their lifetimes from Eq. (43) will be of the order of 2×10^{-12} sec. Such short lifetimes will produce lifetime broadening of the phonon peaks. Just such effects are seen in the neutron scattering.

ACKNOWLEDGMENTS

The authors wish to thank J. L. Slack for help in preparing the CuCl powder, S. Elmå for aid in assembling the pressure cell, and B. Hedman for help with the x-ray analysis. One of us (G.A.S.) also wishes to thank Professor G. Bäckström for his hospitality during a research leave in Sweden and the Swedish Natural Science Research Council for partial support during the course of this research.

[1]G. A. Slack, Phys. Rev. B 22, 3065 (1980).
[2]R. C. Hanson, K. Helliwell, and C. Schwab, Phys. Rev. B 9, 2649 (1974).
[3]T. H. K. Barron, J. A. Birch, and G. K. White, J. Phys. C 10, 1617 (1977).
[4]E. Rappaport and C. W. F. T. Pistorius, Phys. Rev. 172, 838 (1968).
[5]S. V. Popova, N. R. Serebryanaya, and S. S. Kabalkina, Geokhimiya (10)959 (1963).
[6]M. H. Manghnani, W. S. Brower, and H. S. Parker,

Phys. Status Solidi A 25, 69 (1974).
[7]M. Kalliomaki, V. Meisalo, and A. Laisaar, Phys. Status Solidi A 56, K127 (1979).
[8]R. G. Ross, P. Andersson, and G. Bäckström, Mol. Phys. 38, 377 (1979).
[9]O. Sandberg, P. Andersson, and G. Bäckström, *Proceedings of the Seventh Symposium on Thermophysical Properties,* edited by A. Cezairliyan (American Society of Mechanical Engineers, New York, 1977), p. 181.
[10]C. W. Chu, S. Early, T. H. Geballe, A. Rusakov, and R. E. Schwall, J. Phys. C 8, L241 (1975).
[11]C. W. Chu, A. P. Rusakov, S. Huang, S. Early, T. H. Geballe, and C. Y. Huang, Phys. Rev. B 18, 2116 (1978).
[12]C. W. Chu and H. K. Mao, Phys. Rev. B 20, 4474 (1979).
[13]G. J. Piermarini, F. A. Mauer, S. Block, A. Jayaraman, T. H. Geballe, and G. W. Hull Jr., Solid State Commun. 32, 275 (1979).
[14]E. F. Skelton, A. W. Webb, F. J. Rachford, P. C. Taylor, S. C. Yu, and I. L. Spain, Phys. Rev. B 21, 5289 (1980).
[15]G. A. Slack, in *Solid State Physics,* edited by F. Seitz, D. Turnbull, and H. Ehrenreich (Academic Press, New York, 1979), Vol. 34, p. 1.
[16]C. Carabatos, B. Hennion, K. Kunc, F. Moussa, and C. Schwab, Phys. Rev. Lett. 26, 770 (1971).
[17]B. Prevot, B. Hennion, and B. Dorner, J. Phys. C 10, 3999 (1977).
[18]S. S. Jaswal, Solid State Commun. 27, 969 (1978).
[19]Z. Vardeny, G. Gilat, and D. Moses, Phys. Rev. B 18, 4487 (1978).
[20]R. Hill, Proc. Phys. Soc. London, Sect. A 65, 349 (1952).
[21]M. G. Holland, Phys. Rev. 132, 2461 (1963).
[22]P. W. Bridgman, Proc. Am. Acad. Arts. Sci. 67, 345 (1932).
[23]W. Klemm, W. Tilk and S. V. Müllenheim, Z. Anorg. Allg. Chem. 176, 1 (1928).
[24]R. B. Lawn, Acta Crystallogr. 17, 1341 (1964).
[25]H. F. Schaake, as referred to in J. N. Plendl and L. C. Mansur, Appl. Opt. 11, 1194 (1972).
[26]G. Dolling and R. A. Cowley, Proc. Phys. Soc. London 88, 463 (1966).
[27]J. F. Vetelino, S. S. Mitra, and K. V. Namjoshi, Phys. Rev. B 2, 967 (1970).
[28]T. Soma, Phys. Status Solidi B 82, 319 (1977).
[29]W. Richter, J. B. Renucci, and M. Cardona, Solid State Commun. 16, 131 (1975).
[30]Z. Vardeny and O. Brafman, Phys. Rev. B 19, 3290 (1979).
[31]R. Trommer, H. Müller, M. Cardona, and P. Vogl. Phys. Rev. B 21, 4869 (1980).
[32]C. Carlone, D. Olego, A. Jayaraman, and M. Cardona, Phys. Rev. B 22, 3877 (1980).